Q. J. R. Meteorol. Soc. (1998), **124**, pp. 1329–1341

Graupel trajectories and charging: A new numerical approach for cloud electrification studies

By S. MASUELLI*, M. A. PULIDO, C. M. SCAVUZZO and G. M. CARANTI
Universidad Nacional de Córdoba, Argentina.

(Received 2 January 1997; revised 23 June 1997)

SUMMARY

In this work the growth, motion and charging of graupel particles are simulated by computer. The cloud fields are calculated by a three-dimensional cloud model. Another program calculates the time evolution, inside these cloud fields, of graupel properties (size, position, charge and others). The electricity enters both in the charging of the particles through their interactions with other particles and in the motion itself, since in the equation of motion the electrical force is included. Embryos with 500 μm initial diameter are released at 656 locations uniformly distributed in the updraught centre at four altitudes. The trajectories of all the particles are followed all the way to the 0 °C altitude. The graupel is charged by the ice-crystal–graupel non-inductive mechanism.

This kind of approach appears to be a powerful tool to study the electric charging of the graupel in greater detail, since a very high spatial resolution (about 1 m) is easily achieved. Some preliminary analysis of the charges on the precipitation particles is carried out and the results are related to *in situ* observations. For the sake of comparison, trajectories without the electrical interaction are also computed, and it is shown that in some cases the final radius with and without the electrical force can differ by a factor of two to three in either direction depending on the initial position.

KEYWORDS: Cloud microphysics Electrical charge Thunderstorms

1. INTRODUCTION

Measurements inside thunderclouds with significant electrical development have shown that the charge on precipitation particles, when there is an integration over volume, would give rise to the observed electric fields (Dye *et al.* 1986; Weinheimer *et al.* 1991).

Also, it is generally accepted that the charge on these precipitation particles is due principally to ice–ice interactions (Williams 1989). Experimental studies of these interactions (Takahashi 1978; Jayaratne *et al.* 1983; Baker *et al.* 1987; Keith and Saunders 1990; Saunders *et al.* 1991) report that the charge separated during a collision between a small crystal and a graupel depends on the state of the surface of these particles, and then mainly on two environmental parameters: cloud temperature (T) and effective liquid-water content (EW). The sign of the charge on each particle depends principally on these parameters, while the magnitude of the separated charge depends also on the size of the crystal and the relative velocity in the collision (Saunders *et al.* 1991). It should be noted that EW depends on the collision efficiency, which is a function of the terminal velocity and the droplet spectrum, and on the liquid-water content (LWC). For the great majority of collisions the terminal velocity is close to the relative collision velocity.

In order to test the ability of the non-inductive mechanism to reproduce the global electric cloud structure, some numerical models have been developed (Norville *et al.* 1991; Scavuzzo *et al.* 1995; Scavuzzo and Caranti 1996). These studies confirm that the non-inductive crystal–graupel charging is a mechanism capable of producing both quantitatively and qualitatively the main features of thunderstorm electrical structure. This kind of model is built by mapping the electrical variables associated with crystals and graupel particles to a grid that includes all the cloud (with typical grid spacing $\delta x = 250$ m). At each of these points (i, j, k), the electrical parameters are represented by the mean over the particles of one category on a cubic cell 250 m per side.

* Corresponding author: FaMAF–UNC, Ciudad Universitaria, 5000 Córdoba, Argentina.

There is ample evidence that there is a measurable electrical–dynamical interaction in clouds with strong electrical development. As an example Williams and Lhermite (1983) and Zrnic *et al.* (1982) measured changes in particle fall velocities following a lightning discharge when the particles were likely to have been charged and subjected to a strong electric field which diminished suddenly. Sometimes this phenomenon is associated with the rain gush. In general, cloud models do not take into account the electrical interaction on a particle level since it introduces computational complications which are not easily dealt with, or it is not the main interest in their study. In this paper we will show that this interaction cannot be overlooked.

Research on hailstone trajectories within clouds began in the 1970's with Musil (1971), who used a one-dimensional wind field. More accurate trajectories with wind fields from multidoppler radar techniques were developed later (Paluch 1978; Heymsfield 1983; Foote 1984; Knight and Knupp 1986; Miller *et al.* 1990). Alternatively Xu (1983) and Castellano *et al.* (1994) studied trajectories of hailstones using cloud fields from numerical models. These models did not include the electrical effects such as the ones mentioned above. However, those effects are not the only ones. There is also evidence that electricity can act in an indirect way. In fact, electrical parameters are very important in any model as the collision and coalescence efficiencies depend on the charge on the particles as well as on the ambient electric field (Pruppacher and Klett 1978, chapter 14).

The electrical field also affects the growth by changing the terminal velocity of precipitating particles, and therefore the accretion rate. Of course, changes in the growth rate are immediately associated with changes in the trajectories of hydrometeors.

To follow individual particles has the advantage of allowing the understanding of the processes at a finer scale, which is needed to compare with the laboratory results processes which remain masked in a global model. This also allows comparisons of the relative importance of different processes in the growth and electrification of cloud particles, leading to more realistic (more economic) parametrizations for use in global models.

A final motivation to carry out this kind of study arises from a physical standpoint: one usually gains a lot of insight by going back and forth from the macroscopic to the microscopic scales, as can be seen from the kinetic theory example. Thus, the physical connection is clarified. Among previous works in which this method was used, we can quote Paluch (1978), Xu (1983) and Knight and Knupp (1986), who employed stationary wind fields associated mainly with a mature cloud stage, while others (Heymsfield 1983; Miller *et al.* 1990) worked with time-dependent fields. Also, the particles were considered to fall with different drag regimes such as a constant drag coefficient (Paluch 1978) or a drag coefficient deduced from a relationship between the Best and the Reynolds numbers. Generally, the terminal velocity assumption is used. This issue was studied by Castellano *et al.* (1994) where a more complete non-electric motion equation is solved. The common feature in all these works is the absence of electrical influence. However, we must keep in mind that the graupel is generally charged and it is moving inside a strong electric field.

As is evident from the analysis of this literature, these two very closely connected problems (cloud electrification by graupel charging and the simulation of the life of hailstones inside storms) have not been studied in a coupled form. In other words, there are no numerical models of graupel trajectories that include the electrical parameters, with which it would be possible to test these influences on the growth of the graupel, and study the electric evolution of particles inside the thunderstorm with very high resolution.

In this work, we present a numerical model that simulates the trajectories of graupels while they are charged in collision with other ice particles. The trajectory model basically follows previous works (Castellano *et al.* 1994) but with the inclusion of the electric force which depends on the charge of the graupel and the external electric field. The electric

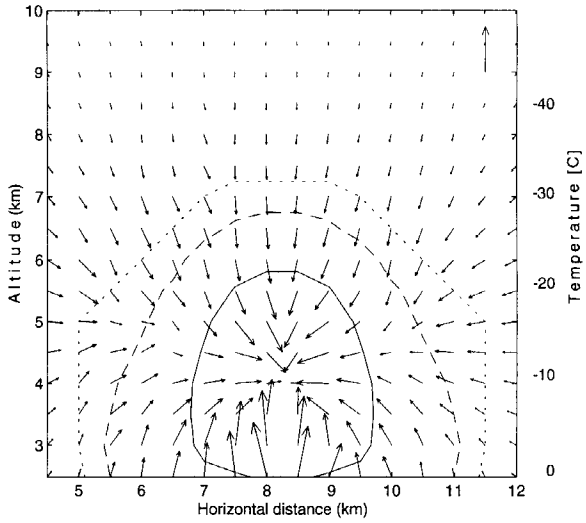

Figure 1. Electric field projection on the *XZ* plane through the cloud centre. The arrow on the right upper corner corresponds to 100 kV m^{-1}. Lines correspond to liquid-water content: solid 2.0 g m^{-3}, dashed 0.5 g m^{-3} and dotted 0.1 g m^{-3}.

charge of the graupel is calculated at each time-step by computing the number of collisions with ice particles present in the cloud and using the experimental data of Saunders *et al.* (1991). This parametrization takes into account all the necessary variables for a detailed description of the electrical evolution of each individual graupel. It is worth mentioning that the concentrations of the ice particles, the external electric field, and the cloud fields (wind, LWC and temperature) are three-dimensional and time-independent as seen in Fig. 1.

In section 2, the complete model is presented. Preliminary analysis of results on the influence of the electric force on the trajectories and the final size of hailstones is presented in section 3, together with an analysis of how the individual charging may end up in the general electrification of the cloud. Finally, in section 4 we present a short discussion and the conclusions.

2. The model

The trajectory and growth of the graupel basically follow the work of Castellano *et al.* (1994). The equation of motion for the graupel particle is assumed to be

$$m \frac{d^2 \mathbf{x}_p}{dt^2} = \mathbf{F}_D - m\mathbf{g} + q\mathbf{E}, \tag{1}$$

where m is the mass of the particle, $\mathbf{F}_D$ is the drag force, $\mathbf{g}$ is the acceleration of gravity, $\mathbf{E}$ is the external electric field and q the charge of the graupel. In Eq. (1), we have added the last term representing the electric force. It is important to note that this equation is an improved approximation over the terminal velocity assumption, since it does not assume instantaneous response. Equation (1) is solved by finite differences using $\Delta t = 0.1$ s. $\mathbf{F}_D$ is given by:

$$\mathbf{F}_D = \left(\frac{C_D\, Re}{24}\right) 6\pi\eta r(\mathbf{U} - \mathbf{V}_p), \tag{2}$$

where Re is the Reynolds number, η is the dynamic viscosity of the air, $\mathbf{U}$ is the wind velocity, and $\mathbf{V}_p$ and r are the particle velocity and radius, respectively. The drag coefficient C_D is given by (Comes *et al.* 1995)

$$C_D = 6.23\, Re^{-0.347}, \tag{3}$$

For each step, the new particle mass is the sum of the mass rate change by accretion and vapour diffusion, in the same form as Castellano *et al.* (1994). In this approach, the wet growth of the graupel is also taken into account.

Density ρ of the growing particles is expressed using Macklin's parameter defined by $x = \bar{r}\, v_0/T_s$, with $\bar{r}$ as the mean volume radius of the cloud droplets, v_0 the droplets impact velocity at the stagnation point and T_s the mean temperature on the particle surface. Following the method given by Levi and Lubart (1991), in the present case, the density is obtained from a set of fittings in terms of Macklin's parameter in the same form as in Castellano *et al.* (1994). Macklin's (1962) formula is used to calculate T_s.

The general structure of the electric part of the model is similar to our previous work (Scavuzzo *et al.* 1995; Scavuzzo and Caranti 1996), but it is adapted to compute the charge on an individual graupel. The graupel particle interacts with other ice particles described by a discrete spectrum (Norville *et al.* 1991; Scavuzzo and Caranti 1996). The spectrum covers a wide range of sizes in eight categories defined in terms of equivalent diameters: (1) 10 μm, (2) 30 μm, (3) 50 μm, (4) 100 μm, (5) 250 μm, (6) 500 μm, (7) 1000 μm and (8) $>$ 5000 μm (Hobbs and Rangno 1985; Weinheimer *et al.* 1991).

The number of collisions between the graupel and the other particles is calculated following a scheme similar to Scavuzzo *et al.* (1995). So, the total number of collisions, per unit time per unit volume, between the graupel and particles 'j' is given by:

$$N_{qj} = \pi R_g^2 E \left| V_{\text{graupel}} - V_{tj} \right| N_j, \tag{4}$$

where N_j is the number density of j-particles, R_g the radius of the larger particle, E the efficiency of the process, and V_{graupel} and V_{tj} the velocities of graupels and particles, respectively. This parameter represents the total probability (event probability) that the collision exists and that the small crystal rebounds, as is considered in the experimental work from the Manchester group (Saunders *et al.* 1991).

The charge separation on each collision basically follows the work by Scavuzzo and Caranti (1996). The charge (δq) transferred to a large particle (diameter D) in an individual collision with a small particle (diameter d) is:

$$\delta q(d, D, EW, T, V) = S(T, EW)R(d, D, EW)M(d, D, EW, T, V), \tag{5}$$

where $S(T, EW)$ determines the sign of the charge transferred, R is a restriction function with values between 0 and 1, V is the actual relative velocity along the trajectory and M is the magnitude of the charge transferred. The sign function S is a function of the reversal temperature $T_r(EW)$ (temperature where the sign of the charge transfer to the graupel changes). As in Scavuzzo and Caranti (1996), the restriction function, R, determines whether or not the charge process is active, now including gradual transitions between these states. Reference to the meaning of this step function can be found in Scavuzzo and Caranti (1996). It is important to consider that in a collision the cases when both particles are larger than 1000 μm or both particles are smaller than 400 μm are excluded in an

attempt to take into account the difference in surface properties of the two interacting particles.

For the magnitude of the transferred charge, the dependence on the size of the colliding particles measured by Keith and Saunders (1989a, 1990) is used in the present model:

$$M(d, D, EW, T, V) = B\, q(T, EW)\, d^a\, V^b, \tag{6}$$

where B, a, b and q are experimental parametrizations given by Saunders *et al.* (1991).

The dependence of the magnitude of the charge transferred during the collision on the velocity of the target (graupel) is defined piecewise assuming a power law V^b, following the experimental data synthesized in Saunders *et al.* (1991) and for velocities larger than 13 m s^{-1} is V^1 (e.g. Caranti *et al.* 1985). To implement the equations of Saunders *et al.* (1991) in a complete form in our model, it is necessary to take into account two parameters which were measured in a variety of conditions by Keith and Saunders (1989b).

One is the effective liquid-water content, defined as the actual liquid-water content that is colliding with the target, because Saunders's diagram is presented in terms of this variable. This parameter is dependent on the collision efficiency of the target in droplet collisions. It is a function of the target size (and its terminal velocity) and the mean size of the cloud droplets:

$$EW = \int_0^\infty ef(r, D, V)\, \frac{4}{3\pi}\, \rho_w\, r^3\, n(r)\, dr, \tag{7}$$

where $ef(r, D, V)$ is the collision efficiency from the formulation of Beard and Grover (1974), ρ_w is the density of water and $n(r)$ is the number of droplets per unit volume between r and $r + dr$. An expression for $n(r)$ based on Wang and Chang (1993) is:

$$n(r) = n_0 * r^2 \exp(-3r/r_m). \tag{8}$$

In turn, the mean radius r_m can be computed from the relationship between $n(r)$ and LWC.

The second parameter mentioned above is the event probability, i.e. the probability that a particle collides and rebounds from the target while separating charge. This will be a function of the sizes of the target and crystal involved in the collision and environmental parameters. In order to include the event probability, we have developed a complete parametrization on the basis of the experimental results presented in Keith and Saunders (1989b). This parametrization includes the dependence on crystal size, the target size and its actual velocity. The values of the event probability ranged between 0.2 to 0.9 depending on the parameters quoted.

The cloud fields (LWC, winds and temperature) are obtained from a 3D numerical cloud model (Scavuzzo and Castellano 1992) in a similar form as in Castellano *et al.* (1994). The chosen fields correspond to one particular time-step belonging to the mature state of the cloud. The electric field is computed from the 3D charge distribution that we obtain using the model described in Scavuzzo and Caranti (1996).

The cloud base formed at height $Z = 2$ km where the temperature was about $T_b = 3$ °C. The 0 °C isotherm is at $Z = 2.5$ km. This cloud is approximately symmetric, since there is no imposed shear, with the updraught centre located at $X = Y = 8.25$ km reaching maximum speeds of 25 m s^{-1}. There are also downdraughts, but they are at distances larger than 3 km from the centre and have maximum speeds limited to 5 m s^{-1}. The general shape of the wind field is that of a slightly asymmetric ascending vortex ring. The electric field reaches 100 kV m^{-1}. The electric field superimposed on contours of LWC on a central XZ plane is presented in Fig. 1.

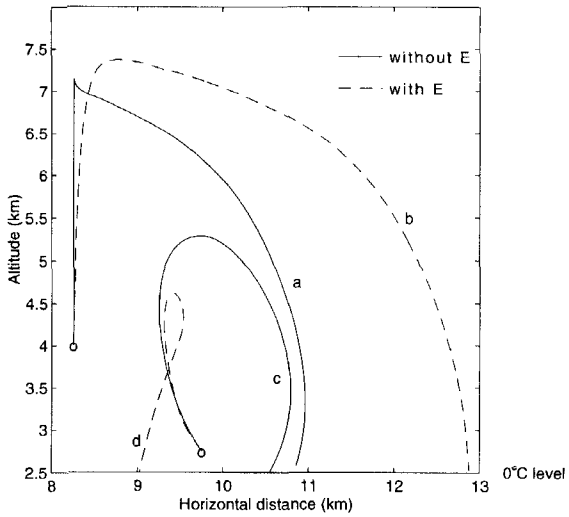

Figure 2. Trajectories projected on the XZ plane from two initial positions, ($X = 8.25$ km, $Z = 4.00$ km) and ($X = 9.75$ km, $Z = 2.75$ km). Solid (dashed) lines correspond to simulation without (with) electric force.

3. Results and discussion

For the sake of brevity, in this work we present only the most important results obtained from the model described in the previous section. A more complete analysis and sensitivity studies of the proposed model will be carried out in a future work.

The results presented below are extracted from a set of 656 trajectories, with 164 different initial positions on each of four horizontal planes ($Z = 2.75$ km, $Z = 4.00$ km, $Z = 5.25$ km and $Z = 6.50$ km). At each one of these planes and separated by $\delta X = \delta Y = 0.25$ km, a regular 'cylindrical' array of embryos (4 km in diameter) centred in the core is released. All the graupel embryos start with $d = 500$ μm and $q = 0$ pC.

The projection of the trajectories on an XZ plane for two initial positions, (8.25 km, 4.00 km) and (9.75 km, 2.75 km), is presented in Fig. 2. For each initial position two trajectories are calculated, one with the electric interaction and the other without it. The effect of taking into account the electrical force in the computation of the trajectory is evident in these cases. For example, both particles without electrical interaction reach the 0 °C isotherm at about the same horizontal region ($X \sim 10.7$ km), while if we include this interaction the same particles reach this isotherm at about $X = 13$ km and $X = 9$ km. In Fig. 2, we can see that due to the inclusion of electrical interactions, some particles are moving outwards and others are moving towards the core of the cloud with important consequences for growth.

In Fig. 3, the evolution of altitude 'Z', diameter 'd' and charge 'q', in a normalized plot is presented as a function of time. Figures 3(a) and (b) present these variables for the pair of trajectories starting at (X, Z) = (8.25 km, 4.00 km) without and with the inclusion of the electrical interaction, respectively. Both particles reach similar maximum altitudes, but the final diameters differ by as much as a factor of three (about 5 mm in case (a) and 1.5 mm in case (b)). Conversely, the final charges are very close (about -200 pC) but with a totally different evolution of this parameter along each trajectory. While the second particle charges negatively in the first 10 seconds and then stops, the first particle alternates periods of negative and positive charging as indicated by the slope of the graph.

Figures 3(c) and (d) present the same kind of plot for the two particles released at (X, Z) = (9.75 km, 2.75 km) without and with electrical interaction included, respectively. In this case, it is the hailstone subjected to the electric force (d) which reaches a larger diameter (3mm in case (c) and 7mm in case (d)). In addition, the charging time dependence is totally different and the particles arrive at the zero isotherm with different signs ($|q| \sim 400$ pC). These examples strongly suggest that the non-inductive charging is indirectly dependent on the electric field through the coupling between the dynamics and the electricity. It should be noted that charge values in this range have been measured inside thunderstorms by Marsh and Marshall (1993) among others.

In the above mentioned results, when the trajectories of graupel are studied for particular cases, the strong effect produced by the inclusion of the electric force in the equation of motion is apparent. This can also be seen in Fig. 4 where, in an attempt to reconcile the above picture with that provided by bulk models and *in situ* measurements, a statistical analysis is presented.

In Fig. 4(a) we present the mean final size for all the graupels arriving at the 0 °C isotherm (considered fall level) at different distances from the cloud core. The averages are computed over four annular regions of 1.5 km width. In turn, Fig. 4(b) shows the final size averaged over all particles departing from four different altitudes with and without E-field. The position and size of the rings as well as the releasing altitudes were chosen somewhat arbitrarily for this figure based only on the geometry of the cloud.

An interpretation of the bar graph in Fig. 4(a) is rooted in the dynamics of the particles. In fact, when released, most particles grow while they are carried upwards by the updraught to regions of divergent flow. Therefore, in the case without an electric field (E-field) the particles tend to be expelled to the periphery of the cloud. The few remaining in the axis grow to very large sizes leading to unlikely large averages in the first ring. On the other hand, when the E-field is taken into account particles are attracted to the axis (due to the positive charge they acquire) where they grow in the high water content of the core. Also, the fact that particles from the periphery (where they grow less) are carried towards the core affects the results by lowering the average size in the first ring.

Figure 4(b) shows that with E-field the general average size is larger than without E-field for each of the chosen releasing altitudes. Particles departing from the 2.75 km level are all located in a convergent flow, high water content and electric field. The charge contributes to move them towards the centre, improving the growth rate with respect to the case without field resulting in a larger average diameter.

The top seeded plane (6.5 km) is quite the opposite. The particles are in a region of divergent flow, weak electric field and low water content, so before they start growing they are ejected to the periphery. Thus both cases lead to similar low average diameter.

The two middle planes are different in the sense that one has to consider them as divided into two or more regions. The particles starting near the axis of the cloud pick up negative charge and are repelled from the centre, while those starting at the outer region pick up positive charge and are attracted. What Fig. 4(b) is showing is that the particles starting outside end up growing more and falling nearer the centre in the electric field case than in the case without field, so much so as to overcome the low performance of the centre particles in the general average.

From these results, we can state that the introduction of the electrical parameters in the calculation of the graupel trajectories is clearly important and cannot be neglected in any way.

Finally, we are interested in obtaining information about the global electrical structure of the cloud from the analysis of the individual trajectories. However, the time information is lost and all we have is a set of complete trajectories, with the associated size and charge

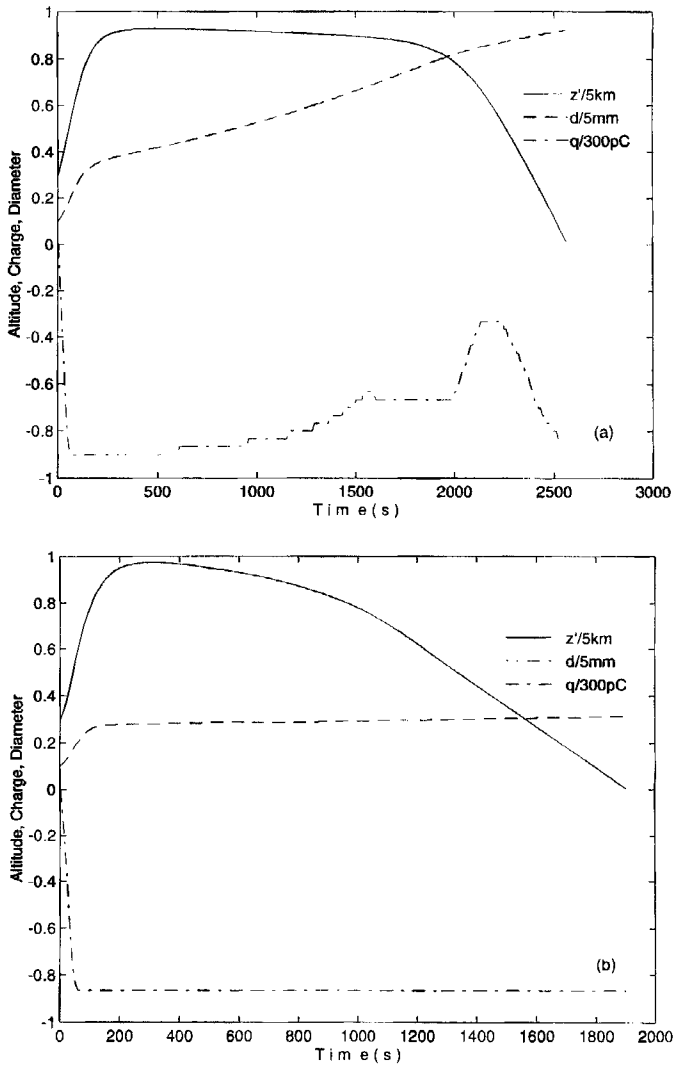

Figure 3. Normalized time evolution of diameters (d, dashed), charge (q, dash dot) and altitude (z', solid) of the four particles (a–d) considered in Fig. 2; z' is the altitude relative to the 0 °C level. In (a) and (b), the vertical axis corresponds to $d/5$ mm, $q/300$ pC and $z'/5.0$ km. In (c) the vertical axis corresponds to $d/7$ mm, $q/400$ pC and $z'/3.0$ km; in (d) the axis is $d/7$ mm, $q/300$ pC and $z'/2.5$ km.

as a function of position along the trajectory. A possible analysis is to categorize these trajectories spatially. For this purpose, the cloud is divided into six regions defined by three adjacent horizontal slabs. These are divided, in turn, into a core region <1.25 km in radius and an annular outer region >1.25 km. The height ranges are 2.5–4.0 km for regions 1 and 2, 4.0–5.5 km for regions 3 and 4, and greater than 5.5 km for regions 5 and 6. Also, inside every region particles are categorized according to their size and charge sign. The size ranges are arbitrarily chosen as: <0.8 mm, 0.8–3.0 mm, and >3.0 mm. In this way, a total of 36 bins are defined.

Although each trajectory is associated with a single particle, it can contribute to different categories simultaneously. For example, a trajectory like d in Fig. 2 lies in four

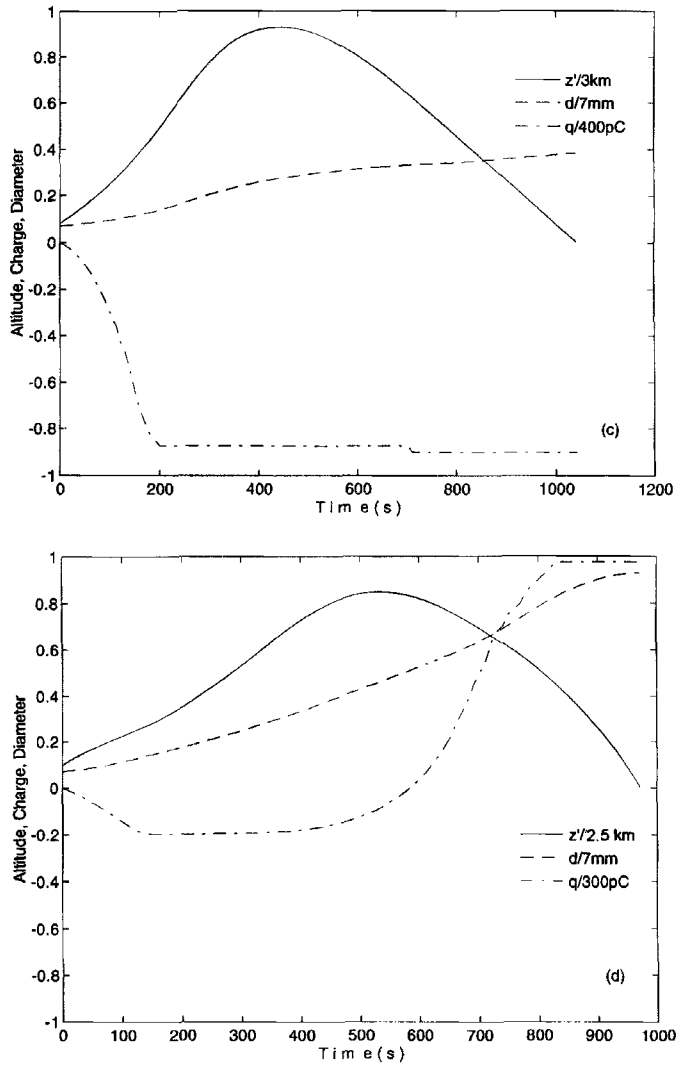

Figure 3. Continued.

regions, and according to Fig. 3(d) it contributes to each of the above-mentioned size and sign bins. Moreover, for the part of the trajectory lying in region 4 (outer middle) it contributes to both signs (see Fig. 3(d) in the abscissa range near 600 s).

Figure 5 presents the results of this analysis. In the lower-level regions 1 and 2 (Figs. 5(a) and (b)), the large particles are essentially positive and the smaller ones are negative in agreement with *in situ* measurements (Marshall and Winn 1982; Weinheimer *et al.* 1991; Marsh and Marshall 1993). At medium altitudes there are fewer larger positive trajectory segments, especially in the inner region where a net negative charge appears in accordance with the negative region expected at this altitude (Williams 1989). At the top of the cloud, the large particles are negative and there is a strong tendency for the small particles to have positive charge. It is important to note that in this study we do not follow ice crystals smaller than 500 μm in diameter. From other numerical studies, we would expect that the positive charge in this region is produced by small ice crystals.

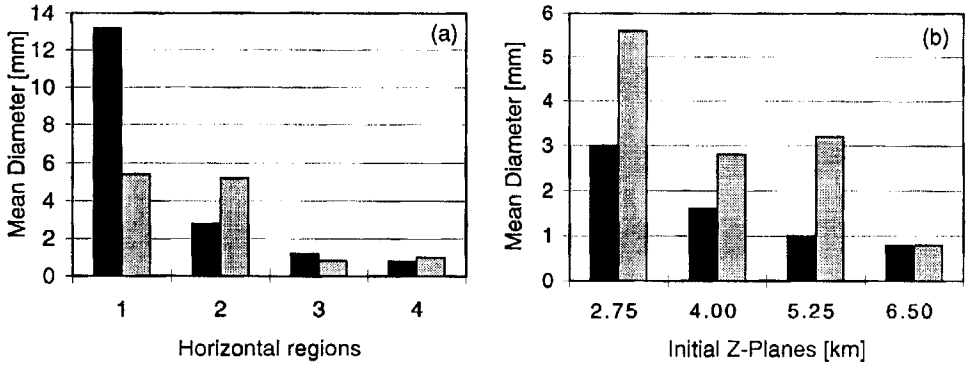

Figure 4. Comparison between final average diameter of graupels with electric force (grey) and without (black). (a) Columns correspond to the average from each of four horizontal annular regions on the 0 °C plane. The first pair of columns corresponds to distances less than 1.5 km from the core, the second to distances between 1.5 km and 3.0 km, the third to 3.0 km and 4.5 km, and the fourth to distances greater than 4.5 km. (b) The final diameter average is taken over all the particles with the same initial altitude. The four pairs of columns correspond to altitude $Z = 2.75$ km, 4.00 km, 5.25 km, and 6.50 km respectively.

4. Conclusions

In this paper we present a model that simulates the growth and charging of the individual graupels inside a thundercloud. This is a novel approach for cloud electrification studies, and represents an improvement due to the incorporation of the electrical effects on the trajectory and growth, which has important consequences. In our opinion, studies like this are a necessary complement to those studies that take the cloud in bulk, and we believe that the potential of the method will give renewed interest to this field of work.

Plots such as those presented in this work (e.g. Fig. 3) represent a very interesting tool to study and identify the more relevant mechanisms of the charging of graupel inside a thunderstorm. While standard numerical electrification models have a typical space resolution of about 100 m, through this approach one can follow the electrical properties of the particles on spatial scales of the order of 1 m with a more complete description of the state of growth of the graupel.

The preliminary results show that the electric effects can produce very large differences in the final sizes in a non-systematic way. This means that coupling the electrical aspects to the microphysics is very important, although it is often a neglected aspect. The dramatic change in the trajectory of graupels is caused by a combination of effects. The particle is attracted or repelled from the water core altering the growth rate, which in turn changes its dynamics. Also, the electrical perturbation on the terminal velocity varies the residence time in a given region, also affecting the growth. This shows that the study of the electrical processes is not only interesting in itself, but also for the strong influence of these processes on the rest of the microphysics, giving more relevance to the study of electrical properties of clouds.

Although the individual charge transfers are not explicitly dependent on the electric field, the charging of the cloud as a whole is influenced significantly by it. The electric field modifies the motion of the particles changing the relative velocity of collision and therefore the individual charge transfer. Moreover, this motion perturbation affects the entire charge separation process in the cloud.

Turning to the global electrification, the charges obtained on graupel, grouped by sizes and zones inside the cloud, are in qualitative agreement with *in situ* measurements

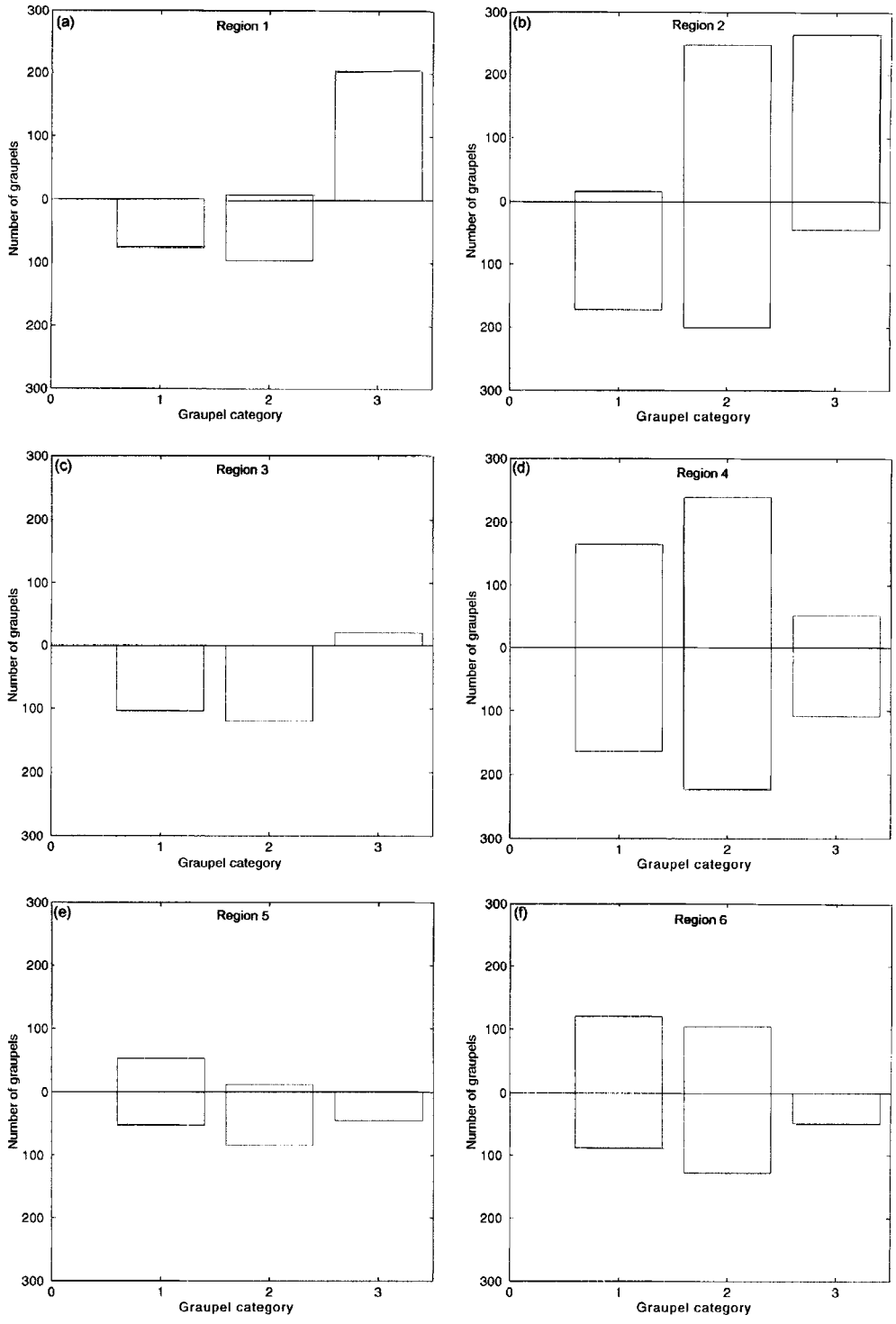

Figure 5. Number of graupels with positive (upward bar) and negative (downward bar) charges at three different altitudes: (a) and (b) below 4.0 km, (c) and (d) 4.0–5.5 km, and (e) and (f) above 5.5 km. (a), (c) and (e) show values from the central region (less than 1.25 km from the cloud centre), and (b), (d) and (f) values from the peripheral region (greater than 1.25 km). Three particle categories are considered: 1—small (less than 0.8 m in diameter), 2—medium (between 0.8 mm and 3.0 mm), and 3—large (greater than 3.0 mm).

(Marshall and Winn 1982; Weinheimer *et al.* 1991; Marsh and Marshall 1993). This is a favourable test for our model and for the particular charging diagram used (Saunders *et al.* 1991). Extensions of this work to other cloud types are necessary before any definite conclusion on the charging diagram can be drawn.

References

Baker B., Baker, M. B., Jayaratne, E. R., Lathan, J. and Saunders, C. P. R. 1987 The influence of diffusional growth rate on the charge transfer accompanying rebounding collisions between ice crystals and hailstones. *Q. J. R. Meteorol. Soc.*, **113,** 1193–1215

Beard, K. V. and Grover, S. N. 1974 Numerical collision efficiencies for small raindrops colliding with micron size particles. *J. Atmos. Sci.*, **31,** 543–550

Caranti, J. M., Illingworth, A. J. and Marsh, S. J. 1985 The charging of ice by differences in contact potential. *J. Geophys. Res.*, **90,** 6041–6046

Castellano, N. E., Scavuzzo, C. M., Nasello, O., Caranti, G. and Levi, L. 1994 A comparative study on hailstone trajectories using different motion equations, drag coefficients and wind fields. *Atmos. Res.*, **33,** 309–331

Comes, R. A., Caranti, J. M. and Krehbiel, P. R. 1995 On the relation of the terminal velocity of hydrometeors to environmental conditions and particle size and density. *Atmos. Res.*, **39,** 69–77

Dye, J. E., Jones, J. J., Winn, W. P., Cerni, T. A., Gardiner, B., Lamb, D., Pitter, R. L., Hallett, J. and Saunders, C. P. R. 1986 Early electrification and precipitation development in a small isolated Montana cumulonimbus. *J. Geophys. Res.*, **91,** 1231–1247

Foote, G. B. 1984 A study of hail utilizing observed storm conditions. *J. Climate Appl. Meteorol.*, **23,** 84–101

Heymsfield, A. J. 1983 Case study of a hailstone in Colorado. Part IV: Graupel and hail growth mechanisms deduced through particle trajectory calculation. *J. Atmos. Sci.*, **40,** 1482–1509

Hobbs, P. V. and Rangno, A. L. 1985 Ice particle concentration in clouds. *J. Atmos. Sci.*, **42,** 2523–2549.

Jayaratne, E. R., Saunders, C. P. R. and Hallett, J. 1983 Laboratory studies of the charging of soft hail during ice crystal interactions. *Q. J. R. Meteorol. Soc.*, **109,** 609–630

Keith, W. D. and Saunders, C. P. R. 1989a Charge transfer during multiple ice crystal interactions with a rimming target. *J. Geophys. Res.*, **94,** 13103–13106

1989b The collection efficiency of a cylindrical target for ice crystals. *Atmos. Res.*, **23,** 83–95

1990 Further laboratory studies of the charging of graupel during ice crystal interactions. *Atmos. Res.*, **25,** 445–464

Knight, C. A. and Knupp, K. R. 1986 Precipitation growth trajectories in a CCOPE storm. *J. Atmos. Sci.*, **43,** 1057–1073

Levi, L. and Lubart, L. 1991 Analysis of hailstones from a severe storm and their simulated evolution. *Atmos. Res.*, **26,** 191–211

Macklin, W. C. 1962 The density and structure of ice formed by accretion. *Q. J. R. Meteorol. Soc.*, **88,** 30–50

Marsh, S. J. and Marshall, T. C. 1993 Charged precipitation measurements before the first lightning flash in a thunderstorm. *J. Geophys. Res.*, **98,** 16605–16611

Marshall, T.C. and Winn, W. P. 1982 Measurements of charged precipitation in a New Mexico thunderstorm: Lower positive charge centres. *J. Geophys. Res.*, **87,** 7141–7157

Miller, L. J., Tuttle, J. D. and Foote, G. B. 1990 Precipitation production in a large Montana hailstorm: Airflow and particle growth trajectories. *J. Atmos. Sci.*, **47,** 1619–1646

Musil, D. J. 1971 Computer modeling of hailstone in feeder cloud. *J. Atmos. Sci.*, **27,** 474–482

Norville, K., Baker, M. and Lathan, J. 1991 A numerical study of thunderstorm electrifications: Model development and case study. *J. Geophys. Res.*, **96,** 7463–7481

Paluch, I. R. 1978 Size sorting of hail in a three-dimensional updraft and implications for hail suppression. *J. Appl. Meteorol.*, **17,** 763–777

Pruppacher, H. R. and Klett, J. D. 1978 *Microphysics of cloud and precipitation.* D. Reidel Publishing Co., Holland

Saunders, C. P. R., Keith, W. D. and Mitzeva, R. P. 1991 The effect of liquid water on thunderstorm charging. *J. Geophys. Res.*, **96,** 11007–11017

Scavuzzo, C. M. and Caranti, J. M. 1996 Thundercloud electrification analysis: the dependence on the temperature–LWC diagram. *J. Atmos. Sci.*, **53,** 349–358

Scavuzzo, C. M. and Castellano, N. E. 1992 'Simulación numérica de procesos atmosfericos: Parte I Modelo de nube'. Pp. 417–426 in *Revista internacional de métodos numéricos para el cálculo y diseño en ingenieria*. Ed. por la Univ. Pol. de Catalunya, España (in Spanish)

Scavuzzo, C. M., Avila, E. E. and Caranti, G. M. 1995 Cloud electrification by fracture in ice–ice collisions. *Atmos. Res.*, **37,** 325–344

Takahashi, T. 1978 Riming electrification as a charge generation mechanism in thunderstorms. *J. Atmos. Sci.*, **35,** 1536–1548

Wang, C. and Chang, J. S. 1993 A three dimensional numerical model of cloud dynamics, microphysics, and chemistry. 1. Concepts and formulations. *J. Geophys. Res.*, **98,** 14827–14844

Weinheimer, A. J., Dye, J. E., Breed, D. W., Spowart, M. P., Parrish, J. L., Hoglin, T. L. and Marshall, T. C. 1991 Simultaneous measurements of the charge, size and shape of hydrometeors in an electrified cloud. *J. Geophys. Res.*, **96,** 20809–20829

Williams, E. R. 1989 The tripole structure of thunderstorms. *J. Geophys. Res.*, **94,** 13151–13167

Williams, E. R. and Lhermite, R. M. 1983 Radar test of the precipitation hypothesis for thunderstorm electrification. *J. Geophys. Res.*, **88,** 10984–10992

Xu, J. 1983 Hail growth in a three-dimensional cloud model. *J. Atmos. Sci.*, **40.** 185–203

Zrnic, D. S., Rust, W. D. and Taylor, W. L. 1982 Doppler spectra lightning and precipitation at vertical incidence. *J. Geophys. Res.*, **87,** 7179-7191